

The 3B/X3 solar flare of 27 February 1992

M.C. López Fuentes¹, C.H. Mandrini¹, M.G. Rovira¹ and P. Démoulin²

¹ *Instituto de Astronomía y Física del Espacio, IAFE, Buenos Aires, Argentina.*

² *Observatoire de Paris, DASOP, Meudon, France.*

Received: November 6, 1998; accepted: April 9, 1999.

RESUMEN

Analizamos la evolución de la región activa (AR) NOAA 7070 y la relacionamos con una fulguración 3B/X3, ocurrida el 27 de febrero de 1992. Las observaciones en rayos X blandos fueron obtenidas por el SXT (Soft X-ray Telescope) a bordo del satélite Yohkoh y las imágenes en H α provienen del Observatorio de Udaipur (India). La ubicación de los núcleos y bandas de la fulguración y la forma de los arcos en rayos X se comparan con el modelo del campo magnético de la AR. Tanto las observaciones como el modelo muestran que los arcos coronales presentan alto "shear" antes de la fulguración y que la configuración se relaja luego de la liberación de la energía. Calculamos la energía magnética libre utilizando el teorema del virial, hallando un límite inferior de 2×10^{32} erg. Este valor concuerda con los valores típicos de energía liberada por estos fenómenos.

PALABRAS CLAVE: Actividad solar, fulguraciones solares, campo magnético solar, magnetohidrostática (MHS).

ABSTRACT

Active region NOAA 7070 was related to a 3B/X3 solar flare that occurred on February 27, 1992. The soft X-ray flare observations were obtained by the SXT (Soft X-ray Telescope) on board the Yohkoh satellite, and those in H α from the Udaipur Observatory. The location of the H α kernels and ribbons, and the shape of soft X-ray loops are compared with the magnetic field model of the AR. Both, observations and model, suggest that the coronal loops are highly sheared before the flare and that the configuration relaxes after energy release. We compute the magnetic free energy at 2×10^{32} erg; this value is typical for the energy released by solar flares.

KEY WORDS: Solar activity, solar flares, solar magnetic field, magnetohydrostatics (MHS).

1. INTRODUCTION

The low resistivity of the coronal plasma allows the long-term allocation of energy in the coronal magnetic field. It is widely accepted that this provides the energy released during solar flares. The relation between magnetic shear and flaring activity is strongly supported by observations (see e.g. Hagyard *et al.*, 1984) and the energy release depends on the active region dynamics and topology. The interaction between coronal structures, forced either by flux emergence or by rapid motions of photospheric structures (see e.g. Mandrini *et al.*, 1991, Démoulin *et al.*, 1994 and Gaizauskas *et al.*, 1998) can create conditions for reconnection.

We discuss the relation between the evolution of the active region (AR) 7070 and the 3B/X3 flare observed on February 27, 1992. In Section 2 we study the white light evolution of the AR. In sections 3 and 4 we analyze the observations of the AR made in H α and soft X-rays during different phases of the flare. In Section 5 we apply a linear non-force free field model to AR7070. The results enable us to estimate a lower limit of the energy of the flare, using the magnetic virial theorem. In Section 6 we provide a phenomenological interpretation of this flare.

2. EVOLUTION OF AR 7070

AR 7070 appeared on the solar disk on Feb. 22, 1992 (Kalman, 1992). It presented a δ -type configuration consisting on two parallel chains of umbrae surrounded by an extensive penumbra. In Figure 1 we show the evolution of the δ configuration and of individual spots. The northern chain consisted of leading (negative) umbrae and the southern chain consisted of following (positive) ones. The neutral line crossed the δ configuration in the East-West direction. On Feb. 23 new magnetic flux emerged. This flux interacted with the old one and a 2B/M4.9 flare was observed. The western spots that belong to the new flux moved at a speed of 84 m/s towards the West between Feb. 23 and Feb. 25. On Feb. 26 their velocity increased to 220 m/s and, on the 27, the 3B/X3 flare was observed. Afterwards, the magnetic flux of the AR started to decrease.

3. H α OBSERVATIONS

The sequence of H α images shown in Figure 2 corresponds to February 27, 1992, during the different phases of the flare. In the first image (5:17 UT), we see the spots of

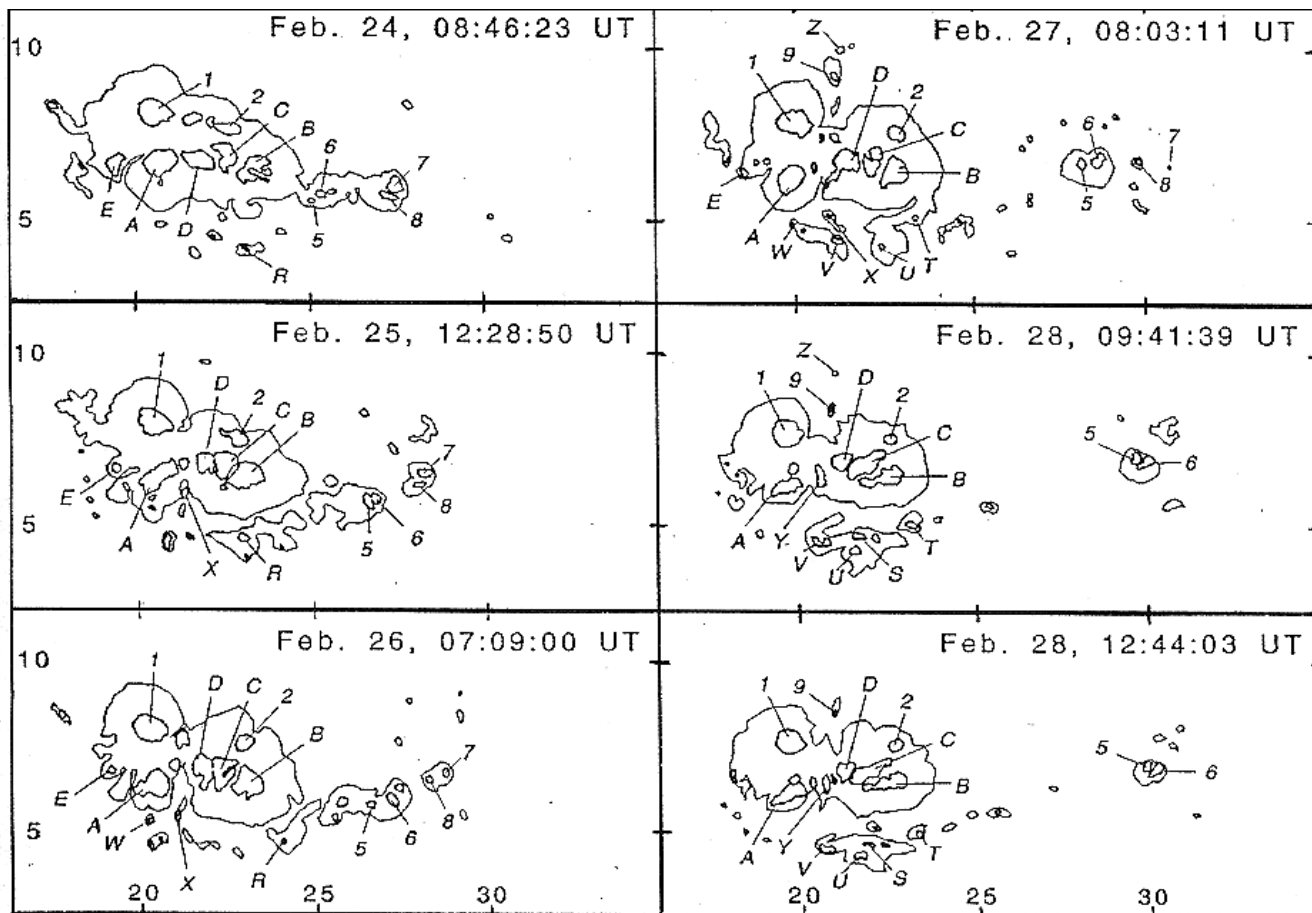


Fig. 1. Evolution of the spots in AR 7070, the big contour corresponds to the δ configuration. The scale is in Carrington coordinates, 1 Carrington degree ≈ 12 Mm. The field of view covers $\approx 96 \times 240$ Mm².

the δ configuration and the filament crossing it in coincidence with the inversion line. The next two images (9:41 and 9:48 UT) show four bright kernels, two on the southern side and two on the northern side of the inversion line. The image at 9:48 UT corresponds to the flare onset observed in hard X-rays and EUV. The maximum emission in H α is observed at 9:56 UT; note the two ribbons of the flare. On this image the filament is not seen. The last two images show the progressive separation of the ribbons. The distance between them is at least 50 Mm, at 11:44 UT.

4. SOFT X-RAY OBSERVATIONS

During the flare onset, Yohkoh was crossing the South Atlantic Anomaly (Brekke *et al.*, 1995), and the working level of its high voltage device was reduced. Because of this, there are no available HXT images, and the SXT images corresponding to the flare onset are saturated. Nevertheless, many non-saturated SXT images were taken during the main phase. Four of these images are shown in Figure 3, outlining the evolution of the coronal arches involved in the event.

The contours superposed on the images indicate the position and shape of the δ configuration. The hot coronal loops appear progressively higher as time goes on. This is consistent with what is observed in H α , where the two ribbons separate from each other. In Figure 4 we show the coronal aspect of the AR before (7:02 UT) and after (16:31 UT) the flare. In the former, the loops close to the inversion line appear to be highly sheared, while in the latter they seem potential.

5. LINEAR NON-FORCE FREE MAGNETIC FIELD MODEL

We apply to AR 7070 the atmospheric magnetic field model developed by Low (1991, 1992, see also Aulanier *et al.*, 1999). This model expresses the current as a function of two components:

$$\nabla \times \mathbf{B} = \alpha \mathbf{B} + f(z) \nabla B_z \times \hat{z} \quad (1)$$

where

$$f(z) = a \exp(z/H) \quad (2)$$

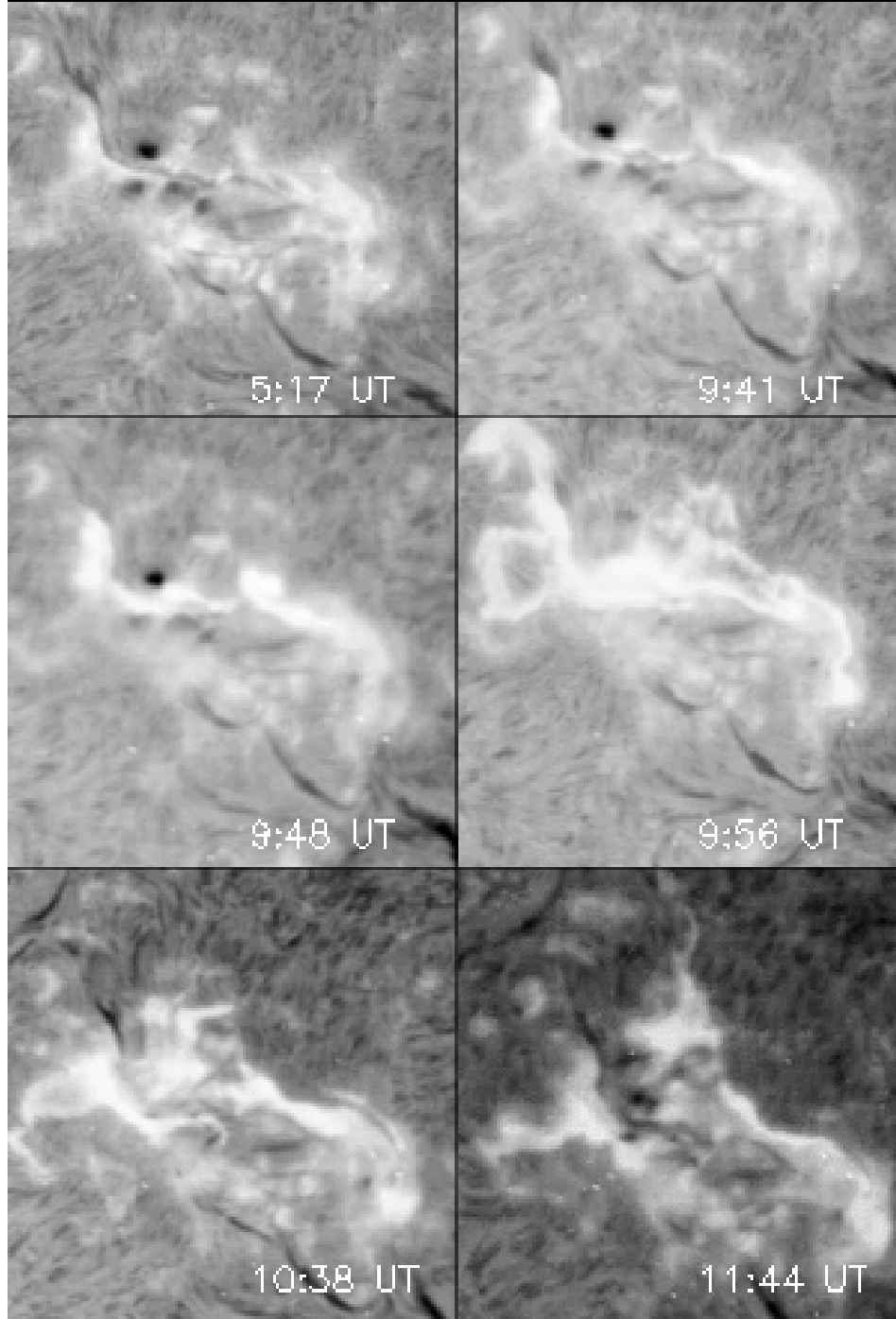


Fig. 2. Sequence of H α images during the flare. In these images North is rotated 15° to the right. The covered field of view on each image corresponds to $\approx 180 \times 180$ Mm 2 .

This last equation together with the MHS equation

$$\frac{1}{4\pi}(\nabla \times \mathbf{B}) \times \mathbf{B} - \nabla p - \rho g \hat{z} = 0 \quad (3)$$

can be solved to give the magnetic field. The plasma pressure and density due to the non-force free condition are respectively:

$$p = p_0(z) - \frac{1}{8\pi} f(z) \mathbf{B}_z^2 \quad (4)$$

$$\rho = \frac{1}{g} \frac{dp_0}{dz} + \frac{1}{4\pi g} \left[\frac{1}{2} \frac{df}{dz} B_z^2 + f(\mathbf{B} \cdot \nabla) B_z \right]. \quad (5)$$

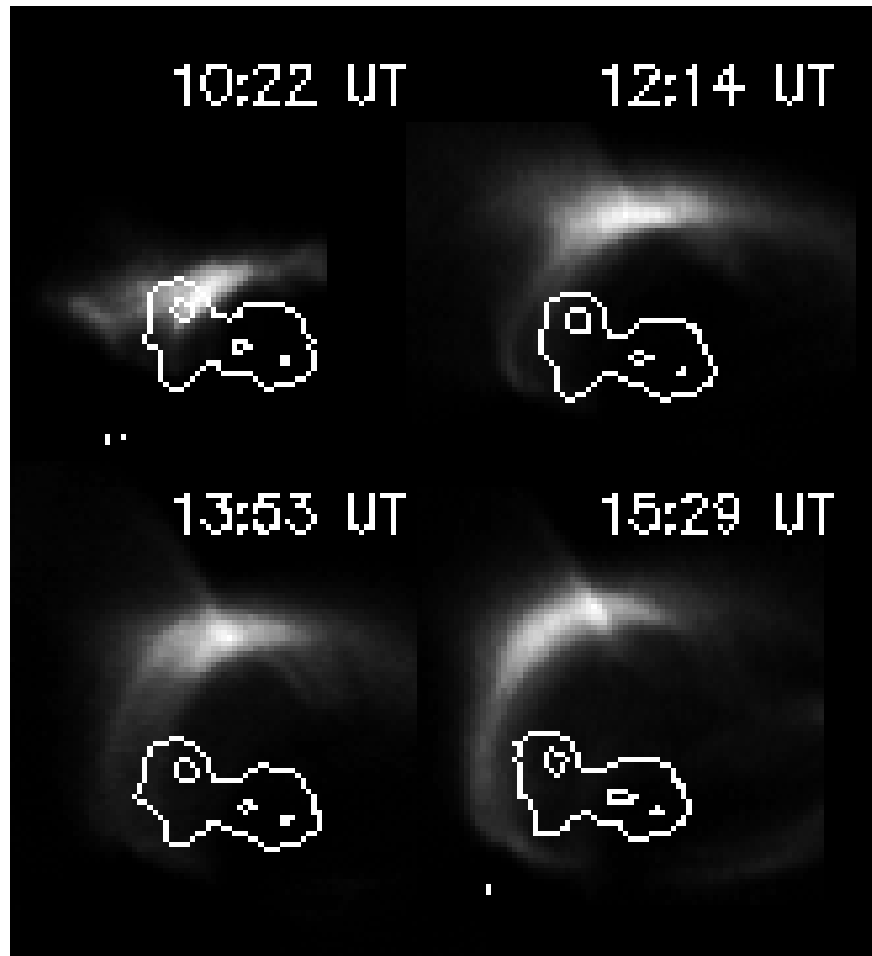


Fig. 3. SXT images showing different stages of the flare gradual phase. The field of view of the images is $\approx 100 \times 100 \text{ Mm}^2$.

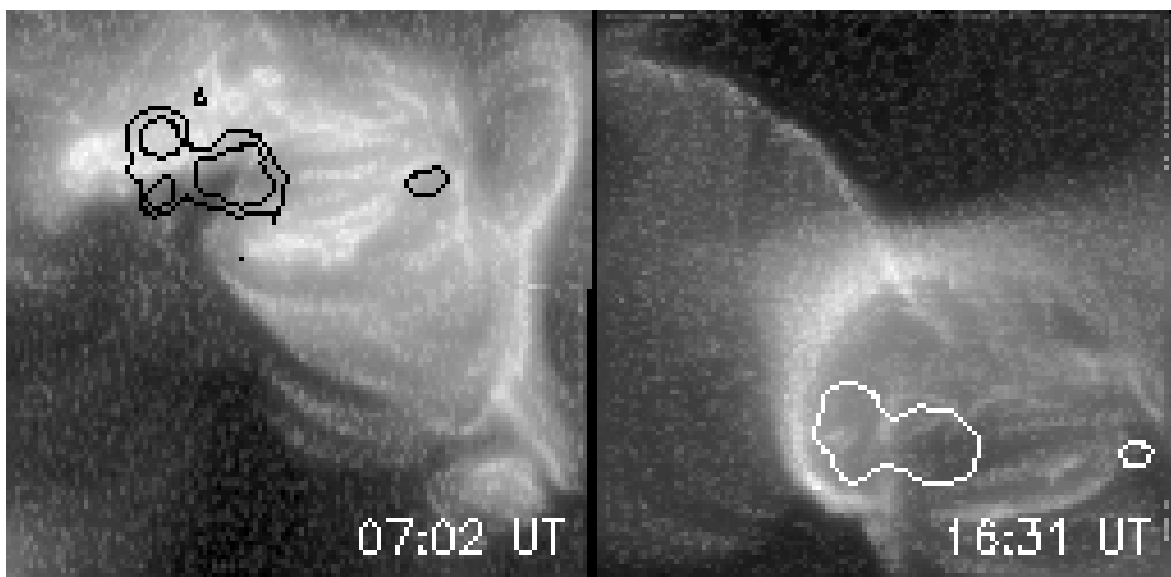


Fig. 4. Comparison of SXT images before and after the flare. North is to the top and West is to the right. The observed field of view is $230 \times 230 \text{ Mm}^2$.

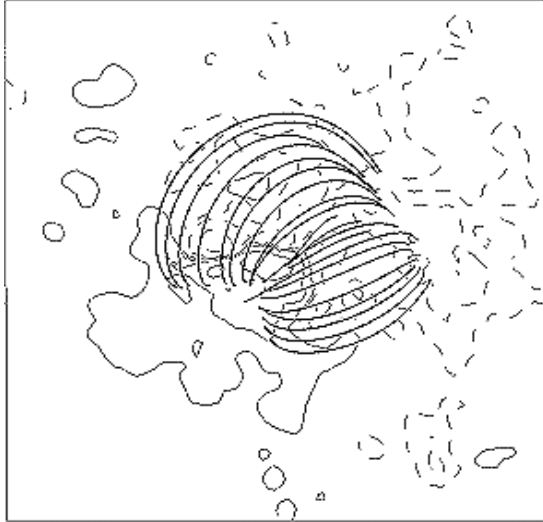


Fig. 5. Extrapolation of the magnetic field in the potential case. The size of the box is $\approx 230 \times 230 \text{ Mm}^2$. The isocontours represent the line of sight magnetic field, corresponding to 100, 500 and 1500 Gauss; positive and negative with continuous and dashed lines respectively.

The results are shown in Figures 5 and 6. The boundary conditions have been taken from a MSFC (Marshall Space Flight Center) magnetogram. Figure 5 corresponds to the potential magnetic field, while Figure 6 shows the change in the field lines with increasing α , i.e. the shear of the magnetic field lines. We have drawn isocontours of the line-of-sight magnetic field. Comparing with X-ray observations, before the flare the coronal loops are consistent with a high α value. After the flare the magnetic configuration can be represented by a potential field. The estimated errors in the overlays between H α and SXT images and the computed maps is about 4 Mm, twice the size of the pixels.

Taking the value of α that best matches the global shape of the soft X-ray loops, we obtain a linear force-free model of AR 7070. Using the magnetic virial theorem we calculate the lower limit of magnetic free energy at $2 \times 10^{32} \text{ erg.}$, since the observed shear is higher than can be modelled with our approximation for the shorter field lines.

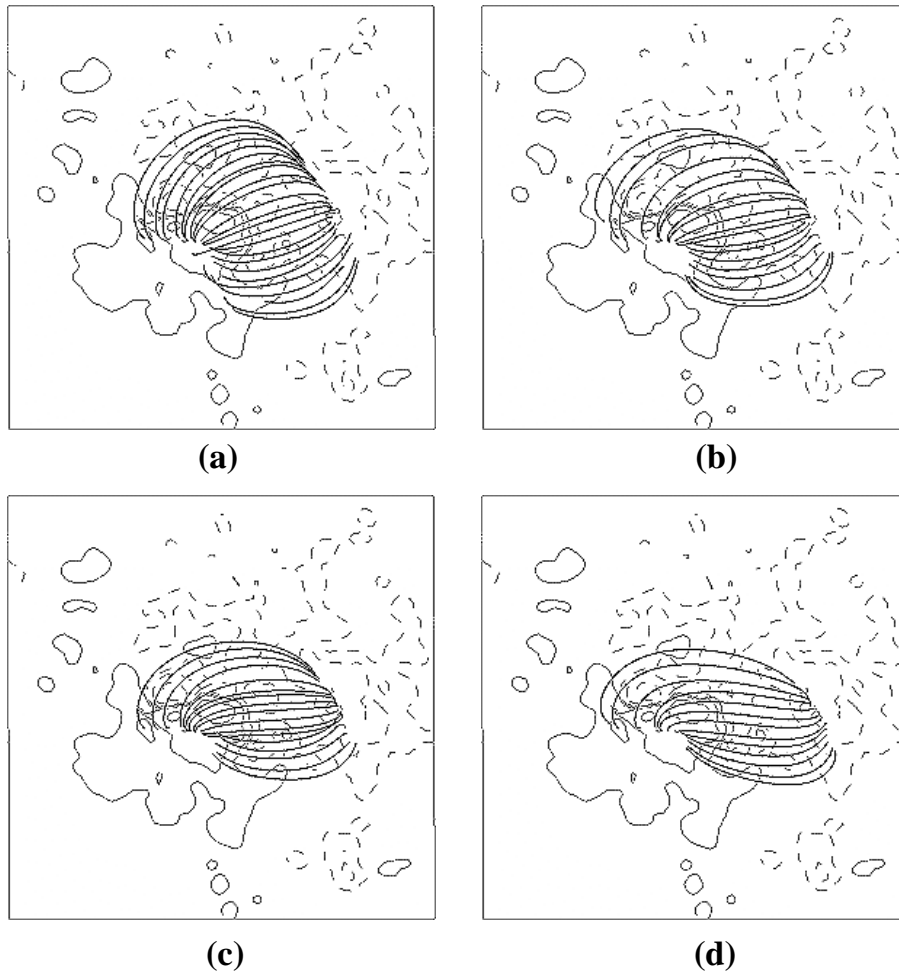


Fig. 6. Extrapolation of the magnetic field for different values of α . The α values for the panels are: a) -0.003 Mm^{-1} , b) -0.006 Mm^{-1} , c) -0.009 Mm^{-1} , d) -0.013 Mm^{-1} . The convention is the same as in Fig. 5.

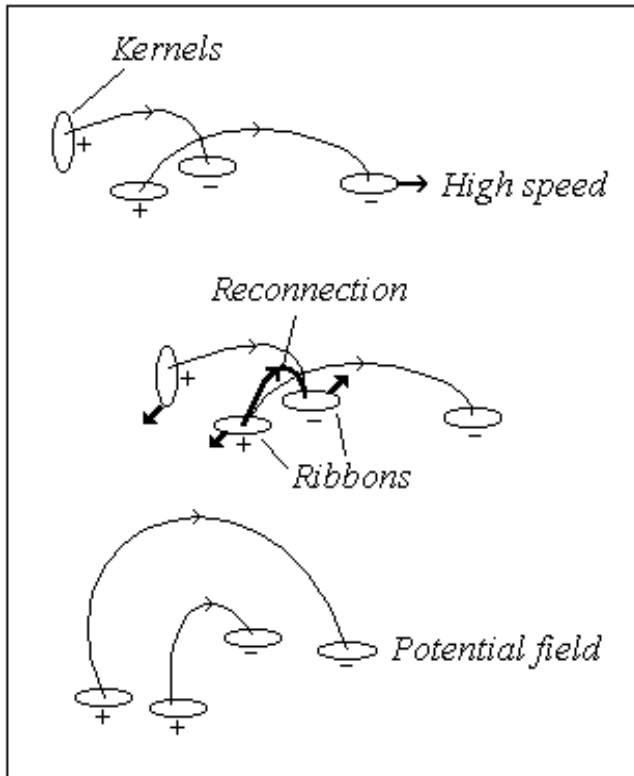


Fig. 7. Phenomenological model for the flare evolution. The rapid displacement of the spots gives place to a magnetic instability.

6. CONCLUSIONS

The studied AR is typical of regions associated with flaring activity. It features magnetic flux emergence, high shear and rapid motions of the photospheric structures. The observed velocity of the western spots coincides with those measured in other flaring active regions (Gaizauskas *et al.*, 1998).

A sketch of the evolution of the flare is shown in Figure 7. The high velocity of the western spots destabilized the configuration, forcing an interaction between the loops connecting the old and new flux. The filament erupted, and we observe the brightening of progressively higher loops due to magnetic reconnection, according to the mechanism proposed by Kopp and Pneuman (1976) and Kopp and Poletto (1984). After energy release, the magnetic field relaxed showing a more potential aspect.

The model represents an improvement over the usual linear force free magnetic field model, because it includes the interaction between plasma and magnetic field due to the Lorentz force. The value obtained for the free energy is within the typical range observed in flares (see e.g. Sakurai *et al.*, 1992, Falewicz and Rudawy, 1999).

ACKNOWLEDGEMENTS

The Yohkoh Team and the MSSL YDAC provided the Yohkoh/SXT data, and the MSFC Vector Magnetograph Group the magnetograms used in this work. We thank L. van Driel-Gesztelyi for instructing us about the use of the Yohkoh software and B. Kalman for the report of the AR7070 white light observations. The authors thank the ECOS-SECYT cooperative science program (A97U01) for financial support.

BIBLIOGRAPHY

- AULANIER, G., P. DEMOULIN, B. SCHMIEDER, C. FANG and Y. H. TANG, 1999. Magnetohydrostatic model of a Bald-Patch flare. *Solar Phys.*, *183*, 369-388.
- BREKKE, P., G. J. ROTTMAN, J. FONTENLA and P. G. JUDGE, 1996. The ultraviolet spectrum of a 3b class flare observed with SOLSTICE. *Astroph. J.* *468*, 418-432.
- DEMOULIN, P., C. H. MANDRINI, M. ROVIRA, J. C. HENOUX and M. E. MACHADO, 1994. Interpretation of multiwavelength observations of November 5, 1980 solar flares by the magnetic topology of AR 2766. *Solar Phys.*, *150*, 221-243.
- FALEWICZ, R. and P. RUDAWY, 1999. X-type interactions of loops in the flare of 25 September 1997. *Astron. Astrophys.*, *344*, 981-990.
- GAIZAUSKAS, V., C. H. MANDRINI, P. DEMOULIN, M. L. LUONI and M. G. ROVIRA, 1998. Interactions between nested sunspots. II. A confined X1 flare in a delta-type sunspot. *Astron. Astrophys.*, *332*, 353-366.
- HAGYARD, M. J., D. TEUBER, E. A. WEST and J. B. SMITH, 1984. A quantitative study relating observed shear in photospheric magnetic fields to repeated flaring. *Solar Phys.*, *91*, 115-126.
- KALMAN, B., 1992, private communication.
- KOPP, R. A. and G. W. PNEUMAN, 1976. Magnetic reconnection in the corona and the loop prominence phenomenon. *Solar Phys.* *50*, 85-98.
- KOPP, R. A. and G. POLETO, 1984. Observational evidence for coronal magnetic reconnection during the two-ribbon flare of 21 May 1980. Eighth International Colloquium on ultraviolet and X-ray spectroscopy of astrophysical and laboratory plasmas, Proc. of IAU Colloq. 86, Doschek, G.A. ed., p.17, Reidel, Dordrecht.

LOW, B.C., 1991. Three-dimensional structures of magnetostatic atmospheres. III. A general formulation. *Astrophys. J.*, 370, 427.

LOW, B.C., 1992. Three-dimensional structures of magnetostatic atmospheres. IV. Magnetic structures over a solar active region. *Astrophys. J.* 399, 300-312.

MANDRINI, C. H., P. DEMOULIN, J. C. HENOUX and M. E. MACHADO, 1991. Evidence for the interaction of large scale magnetic structures in solar flares. *Astron. Astrophys.*, 250, 541-547.

SAKURAI, T., K. SHIBATA, K. ICHIMOTO, S. TSUNETTA and L. W. ACTON. 1992. Flare-related relaxation of magnetic shear as observed with the Soft X-ray telescope of YOHKOH and with vector magnetographs. *PASJ: Publ. of Astronom. Soc. Japan*, 44, L123-L127.

M.C. López Fuentes¹, C.H. Mandrini¹, M.G. Rovira¹ and P. Démoulin²

¹ Instituto de Astronomía y Física del Espacio, IAFE, CC 67, Suc 28, 1428 Buenos Aires, Argentina.

Email: lopezf@iafe.uba.ar

² Observatoire de Paris, DASOP, URA 2080, F-92195 Meudon Cedex, France.